ADAMTS7 Promotes Smooth Muscle Cell Foam Cell Expansion in Atherosclerosis

Allen Chung[1], Hyun K. Chang[1], Huize Pan[1, 2], Alexander C. Bashore[1], Karissa Shuck[1], Caio V. Matias[1], Juliana Gomez[1], Hanying Yan[3], Mingyao Li[3], Robert C. Bauer[1]*

[1]Cardiometabolic Genomics Program, Division of Cardiology, Department of Medicine, Columbia University, New York, NY, USA

[2]Division of Cardiovascular Medicine, Department of Medicine, Vanderbilt University Medical Center, Nashville, TN, USA

[3]Department of Biostatistics, Epidemiology and Informatics, University of Pennsylvania Perelman School of Medicine, Philadelphia, PA, USA

***Correspondence to**
Robert C. Bauer, Ph.D.
630 W. 168th Street, PS10-401,
New York, New York 10032, USA.
E-mail: rcb36@columbia.edu

ABSTRACT

Human genetic studies have repeatedly associated SNPs near the gene *ADAMTS7* with atherosclerotic cardiovascular disease. Subsequent investigations in mice demonstrated that ADAMTS7 is proatherogenic, induced in response to vascular injury, and alters smooth muscle cell function. However, the mechanisms governing this function and its relationship to atherosclerosis remain unclear. Here, we report the first conditional *Adamts7* transgenic mouse in which the gene can be conditionally overexpressed in smooth muscle cells, mimicking its induction in atherosclerosis. We observed that smooth muscle cell *Adamts7* overexpression results in a 3.5-fold increase in peripheral atherosclerosis, coinciding with an expansion of smooth muscle foam cells. RNA sequencing of *Adamts7* overexpressed primary smooth muscle cells revealed an upregulation in the expression of lipid uptake genes. Subsequent experiments in primary smooth muscle cells demonstrated that increased *Spi1* and *Cd36* expression leads to increased smooth muscle cell oxLDL uptake. To uncover *ADAMTS7* expression in human disease, we have interrogated the largest scRNA-seq dataset of human carotid atherosclerosis. This analysis discovered that endothelial cells had the highest expression level of *ADAMTS7* with lesser expression in smooth muscle cells, fibroblasts, and mast cells. Subsequent conditional knockout studies in smooth muscle cells surprisingly showed no change in atherosclerosis, suggesting redundant expression of this secreted factor in the vessel wall. Finally, mice overexpressing *Adamts7* in endothelial cells also exhibit increased atherosclerosis, suggesting that multiple vascular cell types can contribute to ADAMTS7-mediated foam cell expansion. In summary, *Adamts7* is expressed by multiple vascular cell types in atherosclerosis, and ADAMTS7 promotes oxLDL uptake in smooth muscle cells, increasing smooth muscle foam cell formation and peripheral atherosclerosis in mice.

INTRODUCTION

Coronary artery disease (CAD) remains the leading cause of death in the United States[1]. Human genome-wide association studies (GWAS) have proven to be an effective and unbiased approach to discovering novel genomic loci associated with CAD, and GWAS have repeatedly identified the 15q25 locus as a region of interest for CAD[2-5]. This genomic locus harbors the gene A disintegrin and metalloproteinase with thrombospondin motifs 7 (*ADAMTS7*), encoding a secreted matrix metalloproteinase previously implicated in osteoarthritis[6]. After its identification by GWAS, subsequent mouse studies demonstrated that *Adamts7* is proatherogenic as mice with global whole-body *Adamts7* knockout had reduced atherosclerosis[7]. Notably, this reduction in atherosclerosis occurred absent any changes in plasma lipoprotein levels, suggesting that *Adamts7* has a lipid-independent role in atherogenesis[8]. Further mouse models of *Adamts7* have confirmed this proatherogenicity while demonstrating that ADAMTS7 catalytic activity is required for this effect[9,10].

Mechanistic studies of ADAMTS7 have mainly focused on its role in modulating smooth muscle cell (SMC) function, as *Adamts7* knockout and overexpression can alter both neointima formation following vascular injury and SMC migration in ex vivo assays[7,11]. There has recently been an increased appreciation of the role of SMCs in atherosclerosis. Previously, SMCs were thought to be a cell type that solely contributes to forming the fibrous cap. However, advances in single-cell technology employing lineage tracing approaches have revealed that SMCs can undergo phenotypic modulation and acquire macrophage-like characteristics[12]. Additionally, studies in the *Apoe-/-* model of atherosclerosis revealed that the vast majority of foam cells are not macrophages but rather cells of SMC origin, indicating that SMC foam cells play a more significant role in atherogenesis than previously understood[13]. *Adamts7* is not constitutively expressed in vascular cells but rather its expression is induced in SMCs in response to vascular injury and cytokine signaling[7,9]. In mice, *Adamts7* expression is observed at early plaque stages but not in advanced lesions[7]. Although ADAMTS7 has consistently been linked to SMC function, the mechanistic basis by which ADAMTS7 promotes atherosclerosis remains unknown[8].

In this study, we report the first ever tissue-specific *Adamts7* mouse model, allowing for mechanistic studies of ADAMTS7 during sustained induction or knockout in SMCs. We demonstrate that SMC-specific *Adamts7* overexpression increases atherosclerosis, reduces fibrous cap thickness, and increases SMC foam cell formation. We found in primary SMCs that *Adamts7* overexpression increases the expression of the myeloid transcription factor PU.1 and multiple lipid uptake genes, which in turn increases SMC oxidized low density lipoprotein (oxLDL) uptake. Finally, we identify redundant

ADAMTS7 expression in SMCs and endothelial cells (ECs) in humans and demonstrate that EC-specific *Adamts7* expression also increases atherosclerosis. In conclusion, we show that ADAMTS7 promotes SMC foam cell expansion and, ultimately, atherosclerosis.

RESULTS

Overexpression of *Adamts7* in mouse SMCs exacerbates atherosclerosis.

Prior investigations demonstrated that the induction of ADAMTS7 expression has a wide range of effects on vascular SMCs[7,9,11]. Given these findings, we generated a mouse model overexpressing *Adamts7* in SMCs to mimic its induction and promote its function (Figure 1A). The murine *Adamts7* was inserted into the Rosa26 locus with a floxed stop codon preceding the gene, allowing for tissue type-specific overexpression of *Adamts7*. The transgenic overexpression model (TG+) was subsequently bred to the Myh11-CreERT2, allowing for the SMC-specific overexpression of *Adamts7*, and the *Ldlr* knockout background to confer hyperlipidemia[14]. We verified that SMCs overexpress *Adamts7* at both the RNA (Figure 1B) and protein levels (Figure 1C) when compared to mice lacking the transgene (TG-).

To investigate the effects of SMC ADAMTS7 on atherosclerosis, the mice were fed a western-type diet (WTD) for 16 weeks. There was no observable difference in body weight (Figure S1A) or cholesterol levels (Figure S1B) between mouse groups after WTD feeding, indicating that any atherosclerosis phenotype is not blood cholesterol dependent. After 16 weeks of WTD feeding, TG+ mice had a 3.5-fold increase in atherosclerosis as quantified by Oil Red O staining of the en face aorta (Figure 1D). Moreover, even with short durations of WTD, including that of three, six, and nine weeks of WTD feeding, we found increased atherosclerosis at all time points, with the six- and nine-week time points reaching statistical significance (Figure S2).

Adamts7 reduces fibrous cap thickness and SMC content within aortic root lesions.

Interestingly, total lesion area quantification of aortic root sections after 16 weeks of WTD feeding revealed no differences between the TG- and TG+ mice (Figure 1E). To better understand the plaque morphology, we further characterized the composition of the root lesions. We found no changes in the necrotic core area (Figure 1F) or macrophage content via Mac2 staining. However, in TG+ lesions, we observed reduced SMC content via □-SMA staining (Figure 1G), and this lack of □-SMA staining is especially prominent in the cap region. The reduction in □-SMA also coincided with reduced fibrous cap

thickness as assessed through picrosirius red staining (Figure 1H). These findings highlight the adverse role of ADAMTS7 in plaque stability.

Adamts7 promotes foam cell formation.

Given the large increase in Oil Red O staining, we next sought to enumerate and assess foam cells using LipidTOX to stain neutral lipid content within vascular cells. As every cell has lipids, we established the LipidTOX high gate using a normolipidemic C57BL6J mouse to designate the non-foamy population as previously described[13]. After excluding doublets and dead cells, we observed that the TG+ mice contained a 3-fold increase in foam cell content (Figure 2A), mirroring the rise in peripheral atherosclerosis. Further assessment of the foam cells within the aorta revealed that over 80% of these cells were devoid of CD11B and CD64 (Figure 2B), regardless of TG status, consistent with recent findings indicating that most foam cells in atherosclerosis arise from SMCs rather than macrophages[13]. To interrogate if SMCs are the foamy cells within the vasculature, the TG- and TG+ mouse model was subsequently bred to an LSL-ZsGreen reporter to allow for the lineage tracing of SMCs and their derived cells[12]. After 12 weeks of WTD feeding, we assessed the origins of the foam cells. Concomitant staining with the leukocyte marker CD45 revealed that most lipid-laden foam cells were devoid of CD45 and positive for ZsGreen, indicating that *Adamts7* was predominately increasing SMC foam cells (Figure 2C).

To determine if ADAMTS7 promotes SMC foam cell formation through increased lipid uptake, we generated primary SMC explants from the TG- and TG+ mice and treated them with 10ug/mL of DiI-oxLDL for 24 hours. TG+ primary SMCs showed a 38% increase in DiI-oxLDL uptake compared to TG- cells as measured by median fluorescence intensity (MFI) (Figure 2D). Notably, the percentage of positive cells and the degree of staining per cell were both increased within the TG+ cells.

Adamts7 leads to an increase in lipid uptake gene expression in SMCs.

To identify how ADAMTS7 mediates an increase in SMC oxLDL uptake, we performed bulk RNA-seq on SMCs explanted from TG- and TG+ mouse aortas ten days after transgene induction and prior to any WTD feeding (Figure 3A). RNAseq revealed that TG+ cells had increased expression of lipid uptake genes such as *Cd36, Fabp5*, and *Trem2,* and the macrophage-associated marker *Adgre1*. Follow-up qRT-PCR in whole aorta RNA from TG+ mice validated the RNAseq and confirmed that TG+ SMCs had increased lipid uptake and macrophage gene expression (Figure 3B). Ingenuity Pathway Analysis (IPA) on the differentially expressed gene set identified Ingenuity Canonical Pathways enriched within the TG+ SMCs that are typically ascribed to macrophages, such as phagosome

formation and immune signaling (Figure 3C). Overall, the RNA-seq and qPCR data indicate that TG+ SMCs acquire a gene signature typically associated with macrophages, with an enrichment of phagocytic, inflammatory, and lipid-uptake genes, consistent with prior reports that SMCs can upregulate macrophage genes when lipid-loaded[15].

Knockdown of *Cd36* ameliorates enhanced oxLDL uptake conferred by Adamts7.

Given the known role of CD36 as a receptor for oxLDL[16], we further investigated its role in TG+ cells. We corroborated the increase in CD36 in vivo using flow cytometry to stain for CD36 protein in cells from digested TG+/ZsGreen+ aortas after 12 weeks of WTD feeding. ZsGreen+ cells from the TG+ mice had a more significant proportion of cells expressing *Cd36* and an increase in MFI of CD36 signal (Figure 3D), in agreement with the observed in vitro increase in CD36 in TG+ SMCs. Next, we tested whether CD36 was mechanistically responsible for the increase in oxLDL uptake in TG+ cells. siRNA-mediated knockdown of *Cd36* in primary SMCs from TG+ and TG- mice, with wildtype *Ldlr,* reduced the level of *Cd36* expression to the level of the Non-Targeting Control (NTC) of the TG- cells, which could be considered wildtype expression levels (Figure 4A). When oxLDL uptake was assessed, *Cd36* knockdown in TG+ cells mirrored that of NTC-treated WT cells, in agreement with the observed CD36 levels (Figure 4B). These findings establish a mechanistic relationship between Adamts7 and the upregulation of *Cd36* expression, the accumulation of oxLDL, and subsequent SMC foam cell formation during atherosclerosis.

Knockdown of Spi1 in Adamts7 overexpressing SMCs attenuates the expression of macrophage-like and lipid-uptake genes.

We next used IPA to identify upstream regulators that could mediate the observed differential gene expression (Table 1) in TG+ cells. The top predicted activated transcription factor was *Spi1*, which encodes the protein PU.1, a well-described transcription factor critical for the maturation of hematopoietic cells[17]. PU.1 also exhibited a 3.16-fold expression increase in TG+ cells in our RNAseq. To examine whether PU.1 is responsible for the increase in lipid uptake genes, we used siRNA to knock down *Spi1*. Knockdown of *Spi1* ameliorated the increases in gene expression of *Cd36, Fabp5*, *Trem2, Adgre1*, and *Cd68* (Figure 4C). In tandem, we performed siRNA knockdown of the other predicted master regulator transcription factors identified by IPA and found that knockdown of *Cebpa*, *Smarca4*, *Bhlhe40*, and *Klf6* did not ameliorate the increases in lipid uptake gene expression (Figure S3), excluding a role for these transcription factors. Finally, DiI-oxLDL loading of primary TG+ SMCs with *Spi1* knockdown revealed that loss of *Spi1* attenuated the increased oxLDL uptake in TG+ cells

while having no effect in TG- primary SMCs (Figure 4D). This finding indicates that increased PU.1 levels caused by Adamts7 expression are critical for the ability of TG+ SMCs to accumulate lipids.

Adamts7 is induced within multiple vascular cell types during lesion formation

Given the clear role of Adamts7 in modulating SMC function during atherogenesis in mice, we next sought to determine if human atherosclerotic SMCs express *ADAMTS7*. We interrogated the largest human atherosclerotic carotid artery scRNA-seq dataset generated to date[18] and found to our surprise that the strongest *ADAMTS7* expression is in endothelial cells (ECs). There was also *ADAMTS7* expression in SMCs, fibroblasts, and mast cells, but the expression in these cells was much lower than that of ECs (Figure 5A). Given that ADAMTS7 is secreted into the extracellular milieu, this observation suggests potential redundant vascular *ADAMTS7* expression in human atherosclerotic plaques.

We next sought to confirm this observation in mouse models of atherosclerosis. As *Adamts7* expression is induced in response to vascular insult and the expression is transient and waning by terminal time points[7], we first performed RNAscope within the brachial cephalic artery (BCA) of hyperlipidemic *Ldlr-/-* mice at four, six, and nine weeks of WTD feeding to determine when *Adamts7* is expressed during atherosclerosis. We observed *Adamts7* expression at the nine-week timepoint, and this expression was within the developing atherosclerotic neointima and in multiple other locations in the BCA, consistent with expression in SMCs and other cell types (Figure 5B). To confirm EC expression of *Adamts7* in mice, we performed RNAscope in the BCA of *Ldlr-/-* mice after seven and ten weeks of WTD (Figure 5C and Figure 5D). At the seven-week time point, we detected colocalization of the *Adamts7* transcript with *Pecam1*, an EC marker, and at the ten-week time point, both ECs and non-ECs showed expression of *Adamts7*. These data verify that ECs are a cellular source of *Adamts7* expression during atherosclerosis in both mice and humans.

SMC-specific knockout of Adamts7 does not reduce atherosclerosis.

Given the possibility of redundant vascular expression of Adamts7, we next asked if SMC-specific ADAMTS7 is required to promote atherosclerosis. We generated an SMC-specific knockout of *Adamts7* from our previously described knockout mouse[7,19] where exons 5 and 6 are floxed. (Figure 6A). This conditional knockout mouse was bred to the Ldlr-/- background and Myh11-CreERT2, allowing for the tamoxifen-inducible deletion of *Adamts7* in SMCs. Mice were intraperitoneally injected with tamoxifen to delete SMC *Adamts7* and fed WTD for 16 weeks. We observed no change in the atherosclerotic lesion area of the en face aorta of *Adamts7* CKO mice compared to controls (Figure 6B). While a vast body of literature demonstrates *Adamts7* induction in SMCs[7,9,11,20], ADAMTS7 is a secreted metalloproteinase

and as such, the cell type that responds to ADAMTS7 (SMCs) does not necessarily have to be the cell type responsible for producing ADAMTS7. Therefore, this lack of difference in the SMC conditional knockout confirms redundant compensatory *Adamts7* expression in other vascular cell types.

Transgenic endothelial cell *Adamts7* increases peripheral atherosclerosis and foam cell formation

As RNAscope of atherosclerotic mice and scRNA-seq of human carotid atherosclerosis indicated that ECs are a source of *Adamts7*, we bred the TG+ mice to the tamoxifen-inducible EC-specific Cre, the Cdh5-CreERT2 to allow for the EC-specific overexpression of *Adamts7*. We compared atherosclerotic burden in ADAMTS7-TG+, LDLR-/-, Cdh5-CreERT2+ (ECTG+) and ADAMTS7-TG+, LDLR-/-, Cdh5-CreERT2- (ECTG-) mice after *Adamts7* induction with tamoxifen and 16 weeks of WTD feeding. We observed no changes in plasma cholesterol nor body weight (Figure 6C) between the two groups. However, similar to the SMC overexpression of *Adamts7*, ECTG+ mice had an increase in peripheral atherosclerosis when compared to ECTG- mice (Figure 6D). The ECTG+ had increased foam cell content (Figure 6E) and, importantly, the majority of these foam cells (74%) were devoid of CD45, indicating that macrophages are not the major source of foam cells (Figure 6F) and aligning with the findings from mice with SMCs-specific *Adamts7* overexpression. In summary, *Adamts7* expression in the vasculature, regardless of the cellular source, promotes peripheral atherosclerosis and SMC foam cell expansion.

DISCUSSION

GWAS of CAD have revealed over 300 genomic regions associated with the disease[2,21]. However, functional studies to elucidate the precise mechanisms of these targets are still in their infancy. In 2011, our group and others reported the discovery of ADAMTS7 as a gene of interest for CAD[4]. Subsequent GWAS studies have replicated this signal, and even when patient groups are stratified based on ethnicity, this signal remains[21], highlighting its robustness in CAD. Further studies in mice showed that ADAMTS7 is proatherogenic and that its atherogenicity is conferred from its catalytic function[7,9]. Despite the large body of prior work on Adamts7, there have been no tissue-specific in vivo studies of Adamts7 to date. Here, we report a novel mouse model where *Adamts7* can be genetically overexpressed in a cell-specific manner. In this novel model, we demonstrate that SMC Adamts7 is proatherogenic and promotes SMC foam cell formation via increased expression of *Spi1* and *Cd36*.

Adamts7 has low overall expression across most cell types in the basal state. In primary SMCs, *Adamts7* must be induced to confer a detectable migration phenotype[7], making it difficult to study the

downstream consequences of ADAMTS7 function. Our novel mouse model with inducible expression allows for a deeper description of the functional consequences of *Adamts7* expression in SMCs, and we find that constitutive *Adamts7* expression drives large scale gene expression changes leading to increased SMC oxLDL uptake. These changes are largely mediated by increased expression of *Spi1*, which codes for the PU.1 transcription factor, long recognized as a mediator of hematopoietic lineage commitment. A critical remaining knowledge gap is the mechanism by which *Adamts7*, a secreted factor, upregulates the SMC expression of *Spi1*. As the proatherogenicity of *Adamts7* is conferred by its catalytic activity, presumably the cleavage of some extracellular substrate by Adamts7 leads to outside-in signaling and downstream induction of *Spi1*. ADAMTS7 substrates have been proposed in previous studies, but none have been tested in the context of SMC foam cell formation, and the precise cleavage substrate mediating *Adamts7* proatherogenicity remains elusive.

Although macrophages have historically been thought to be the source of foam cells in atherosclerotic lesions, it is increasingly appreciated that SMCs constitute the majority of foam cells in atherosclerosis[13]. When *Adamts7* is induced in the vasculature, SMCs increase their expression of genes involved in lipid uptake, inflammation, and phagocytosis, a gene expression profile reminiscent of a macrophage. Recent studies have definitively shown that SMCs do not contribute to the pool of atherosclerotic macrophages, and thus, we posit that these TG+ SMCs are modulated SMCs with increased lipid uptake capacity[22]. Of these lipid uptake genes, one of the most significantly upregulated genes was *Cd36*. CD36 is a well described receptor for oxLDL, and our studies demonstrate that CD36 is largely responsible for the SMC foam cell phenotype in TG+ mice[16]. In addition, upstream regulator analysis of primary SMCs indicates that *Spi1* is significantly upregulated[23], and knockdown of this hematopoietic transcription factor in SMCs ameliorates the increase in lipid handling gene expression and macrophage markers. These observations suggest that PU.1 may be a critical factor in driving the production of foamy SMCs in vivo, and future studies of SMC PU.1 may help reveal disease-relevant consequences of foamy SMCs.

Despite the substantial body of literature connecting SMCs with ADAMTS7, our SMC conditional knockout mouse did not reveal a change in peripheral atherosclerosis[7]. Our analysis of the most extensive carotid single-cell data set to date highlights that SMCs and other cell types, including ECs and mast cells, all express *ADAMTS7*[18]. As ADAMTS7 is a secreted protein, the cells that respond to ADAMTS7 do not necessarily have to produce *ADAMTS7*. In agreement with this, our mouse model with EC-specific *Adamts7* overexpression has increased foam cell formation, mimicking the SMC-

specific transgenic mouse. Thus, vascular ADAMTS7 promotes the expansion of foam cells, and the expression of *Adamts7* is redundant across multiple cell types within the vasculature.

Overall, ADAMTS7 increases the uptake of lipids within SMCs, thus generating a pronounced atherosclerosis phenotype in mice. While the specific role of SMC foam cells in atherosclerosis remains unclear, it has been reported that SMC foam cells and macrophage differ in their intracellular lipid metabolism[24,25]. While more investigations are required to understand the inherent differences between SMC and macrophage-derived foam cells, lipid-laden, foamy macrophages tend to be less inflammatory[26], and by becoming foamy, these macrophages may no longer contribute to the inflammatory cycle associated with atherosclerosis, raising the possibility that foamy macrophages are beneficial in atherosclerosis. Conversely, we observed reduced fibrous cap thickness with *Adamts7* overexpression. As one well described role of SMCs is the formation of the fibrous cap, it is possible that foamy SMCs cannot stabilize lesions, raising an intriguing scenario where macrophage foam cells are beneficial whereas SMC foam cells are detrimental. Prior studies in mice and humans have linked ADAMTS7 to reduced plaque stability[27,28], and our findings here provide a possible mechanistic explanation for this observation.

In conclusion, our investigation using novel mouse models revealed that ADAMTS7 promotes SMC foam cell formation and atherosclerosis while reducing plaque stability. Our mechanistic studies show that ADAMTS7 stimulates SMCs to uptake lipids in a process dependent on PU.1 and CD36. Contrary to previous assumptions, our conditional knockout model reveals that SMCs are not solely responsible for producing Adamts7. Via the integration of carotid atherosclerosis scRNAseq and RNAscope within atherosclerotic mice, we have identified that ECs are an alternative source of ADAMTS7 in the vasculature. These studies elucidate novel mechanisms governing ADAMTS7 proatherogenicity and link human GWAS to the emerging research of SMC foam cells.

ARTICLE INFORMATION

Acknowledgments

We would like to thank Dr. Muredach P. Reilly for guidance on the execution of these studies. We'd also like to thank the staff of the Columbia Stem Cell Initiative Flow Cytometry Core Facility, under the leadership of Michael Kissner, at Columbia University Irving Medical Center, for their contributions to the work presented in this manuscript. We would also like to thank Dr. Carol Troy for providing the Cdh5-CreERT2 mice.

Sources of Funding

A.C. is supported by American Heart Association Predoctoral Fellowship No. 909206. H.P. is supported by National Institute of Health (NIH) grants 5K99HL153939 and R00HL153939. A.C.B. is supported by the NIH Postdoctoral Training in Arteriosclerosis fellowship 5T32HL007343. K.S. is supported by NIH Training in Cellular, Molecular and Biomedical Studies 5T32GM145766. M.L. is supported by NIH grant Nos. R01GM125301, R01HL113147, R01HL150359, and R21HL156234. R.C.B. is supported for this work by NIH grant Nos. R01HL141745 and R01DK134026.

Disclosures:

None

Nonstandard Abbreviations and Acronyms

A disintegrin and metalloproteinase with thrombospondin motifs 7 (ADAMTS7)
Brachial Cephalic Artery (BCA)
Coronary Artery Disease (CAD)
Endothelial Cells (ECs)
Genome-wide association studies (GWAS)
Ingenuity Pathway Analysis (IPA)
Lox-Stop-Lox (LSL)
Median Fluorescence Intensity (MFI)
Oxidized low-density lipoprotein (oxLDL)
Single Cell RNA sequencing (scRNA-seq)
Smooth Muscle cells (SMCs)
Western Type Diet (WTD)

MATERIALS AND METHODS

Animals

All animal studies described were approved by the Institutional Animal Care and Use Committee at Columbia University under protocol AABU8650. C57BL/6J (Stock:000664), Ldlr KO (Stock: 002207), ZsGreen (Stock: 007906), and Myh11 CreERT2 (Stock: 019079) were purchased from the Jackson Laboratory and bred in our laboratory. *Adamts7* knockout mice were previously described[7]. The Cdh5-CreERT2 Mouse was developed by the laboratory of Ralf Adams and has been previously described[29].

To generate a floxed *Adamts7*, the *Adamts7* knockout mouse (MMRRC:046487), was bred to a FLP recombinase mouse. *Adamts7* transgenic mice were created by cloning the mouse allele of *Adamts7* into the pR26 CAG/GFP Asc plasmid. pR26 CAG/GFP Asc was a gift from Ralf Kuehn (Addgene plasmid # 74285). Subsequently, the FL19 embryonic stem cells were used to generate chimeras, which were then crossed to the C57BL6J background. As the Myh11-CreERT2 was inserted into the Y chromosome, only male mice were used for this study. For CreERT2 activation, tamoxifen (Sigma-Aldrich: T5648) was dissolved in 90% corn oil and 10% ethanol; subsequently, mice at seven weeks of age were injected with tamoxifen for five days at a dosage of 40mg/kg of body weight per day. At eight weeks of age, the mice were fed a western diet consisting of 40% Kcal by fat and 0.15% Cholesterol (Research Diet: D12079Bi). For blood collection, mice were fasted for four hours and subsequently sedated with isoflurane, and blood was collected by retroorbital puncture with heparinized microcapillary tubes. Plasma was isolated by centrifugation at 1500 RCF for 10 minutes at 4C. Total cholesterol was measured using the Infinity Cholesterol Reagent (Thermo Scientific: R22421).

Atherosclerosis analysis

For atherosclerosis studies, mice were sacrificed by cervical dislocation and perfused with PBS. The aorta was dissected and subsequently fixed in 10% formalin. Whole aortas were stained with Oil Red O. Hearts containing the aortic root were fixed in 4% paraformaldehyde for 24 hours, transferred to 70% ethanol, and embedded in paraffin wax. Sectioning was performed using a Leica microtome at 8um thickness. The heart was sectioned from the inferior heart towards the aortic root. 25 slides were collected, with each slide containing two sections. We aimed to have the breakage of the leaflet occur on slide 13. Slides 3, 8,13,18, and 23 were used hematoxylin and eosin staining to allow for lesion size quantification. Hematoxylin and Eosin, and Picrosirius Red staining was performed at Columbia's Molecular Pathology Shared Resource.

Immunofluorescence

Immunofluorescence was performed on paraffin sections of the aortic root. Deparaffinization was performed using xylene. Antigen retrieval was performed using a citrate-based agent. Sections were subsequently blocked using 10% normal goat serum for at least one hour. Subsequently, the sections were stained using the following antibodies and dilutions 1:1000 αSMA-Cy3 (Sigma Aldrich: C6198), 1:500 Mac2. IgG controls were purchased from Jackson Immunoresearch. The sections were washed with PBS containing 0.01% Tween 20. For the secondary antibody, a donkey anti-rabbit Alexa Fluor 647 (Invitrogen: A-31573) and goat anti-mouse Alexa Fluor 546 (Invitrogen: A-11030) were used, both at a 1:1000 dilution in 1% goat serum. The slides were washed and mounted with ProLong Glass

Antifade Mountant with NucBlue Stain. Imaging was conducted on a Nikon Eclipse Ti-S microscope, and image processing was performed using ImageJ.

Vascular SMC isolation for tissue culture

SMC isolation was isolated as previously described[30]. The aorta was dissected from the ascending arch to the diaphragm and was predigested for 10 minutes at 37°C with 175U/ml Collagenase II and 1.25U/ml elastase in HBSS to allow for the removal of the adventitia. After removing the adventitia, the media layer was further digested in 400U/ml collagenase II, 2.5U/ml elastase, and 0.2mg/ml soybean trypsin inhibitor at 37°C for one hour in a rotating incubator. The cells were cultured in DMEM supplemented with 20% fetal bovine serum, 1% L-Glutamine, 1% sodium pyruvate, and 1% Penicillin Streptomycin. Cells between passages two and seven were used for experiments.

Vascular SMC isolation for flow analysis

Mice were sacrificed and perfused with PBS. The ascending aorta to the bifurcation at the common iliac artery was dissected and digested with a cocktail consisting of 4 U/mL Liberase TM (Sigma-Aldrich: 5401127001), 60 U/mL hyaluronidase (Sigma-Aldrich: H3506), and 60 U/mL DNase I (Worthington Biochemical Corporation: LS006333) in RPMI-1640. The digestion enzymes were neutralized with 10% FBS in RPMI and washed once in FACS buffer (2% FBS, 5 mM EDTA, 20 mM HEPES, and 1 mM Sodium Pyruvate in DPBS). Cells were then blocked with TruStain FcX PLUS (anti-mouse CD16/32) (Biolegend: 156603) for 10 mins at 4°C. Staining was performed in FACS buffer at the following dilutions: 1:1000 LipidTox Red (Thermo Scientific: H34476), 1:100 CD36 Super Bright 600 (Invitrogen: 63-0362-82), 1:200 CD45-Alexafluor700 (Biolegend: 157209). Cell viability was assessed with DAPI

In vitro cell culture experiments

For In vitro foam cell analysis, cells were treated with DiI conjugated oxLDL (Invitrogen: L34358) at a concentration of 10ug/mL for 24 hours. Subsequently, they were washed with PBS and detached using 0.25% Trypsin EDTA. Neutralization of trypsin was performed using FACS buffer. The cells were counterstained with DAPI to assess live cells, and all analysis was done using either a Novocyte Quanteon or Penteon. For siRNA experiments, all siRNAs were purchased from IDT. Transfection was performed using RNAimax according to the manufacturer’s protocol. All siRNAs were used at a concentration of 10nM.

RNA Isolation and Quantitative RT-PCR

For tissue samples, specimens were collected in Trizol and homogenization was performed using a tissue lyser (Qiagen). The RNA was extracted using the Direct-zol RNA MiniPrep Kit (Zymo) according to the manufacturer's instructions. For cells, RNA was collected using the Quick-RNA Microprep Kit (Zymo). Complementary DNA was synthesized using High-Capacity cDNA Reverse Transcription Kit (Applied Biosystem). All qPCR was performed using TaqMan probes and performed on the Applied Biosystems QuantStudio 7 Flex Real-Time PCR System. Analysis was performed using the 2-DCCT Method.

RNAscope

RNAscope was performed on sections of mouse BCAs after specified durations of WTD feeding. The BCAs were freshly frozen and sectioned at 8um thickness. RNAscope was performed according to the manufacturer's instructions. The sections were first fixed in 10% neutral buffered formalin. Subsequently, the sections were dehydrated and treated with hydrogen peroxide and protease. Hybridization with *Adamts7* (Advanced Cell Diagnostics: 533341) and *Pecam1* (Advanced Cell Diagnostics: 316721-C3) probes was performed. After probe hybridization, hybridization with AMPs 1-3 was performed. Signal development was conducted using Akoya Biosciences Opal Reagent Kits, and slides were mounted using Prolong Glass Antifade Mountant (Thermo Scientific: P36984). Imaging was conducted on a Nikon Eclipse Ti-S microscope, and image processing was performed using ImageJ.

Western Blot

Samples were lysed in RIPA buffer (Thermo Scientific) supplemented with 1% Halt Protease and Phosphatase Inhibitor Cocktail. Tissue samples were lysed with the Qiagen TissueLyser and samples were subsequently cleared by centrifugation at 20,000 RCF for 10 minutes at 4C. Samples were denatured, resolved on a 4-12% Bis-Tris gel, and transferred to either PVDF or a nitrocellulose membrane. Blocking was performed with 5% milk, and primary antibodies were diluted 1:1000 in 5% milk and incubated overnight at 4C. Membranes were washed with 0.1% TBST and probed with the appropriate secondary antibody for one hour at room temperature. Membranes were visualized with ECL using the Amersham Imager 600 gel imager.

Statistical Analysis

Statistical tests can be found in the figure legends. Between sample comparisons were through unpaired 2 tailed t test in GraphPad Prism 10. $P < 0.05$ was considered significant. ANOVA analysis with multiple correction was used for comparison between multiple groups using Sidak's post analysis

as indicated in the figure legends. qPCR results are presented as mean +/- standard error of the mean. All other data is presented as mean +/- standard deviation.

FIGURE LEGENDS

Figure 1. SMC Transgenic *Adamts7* increases atherosclerosis. A, Schematic overview of the generation of the SMC Transgenic ADAMTS7 mouse. Created with BioRender.com B, Verification of *Adamts7* overexpression by qPCR n = 3 mice. C, Validation of ADAMTS7 protein overexpression n = 4 mice. D, Representative images of en face Oil Red O stained aortas and quantification of lesion area n = 5 mice. E, Representative images of hematoxylin and eosin (H&E) stained aortic root sections, quantification of plaque areas n = 6 mice. F, Representative images of hematoxylin and eosin (H&E)-stained aortic root sections with necrotic core outlined in dotted line n = 6 mice. G, Representative images of aortic root sections stained against smooth muscle cell α-actin (Cy3 - red), Mac2 (AlexaFluor 488 - green), and cell nuclei (DAPI - blue) with their subsequent quantification relative to lesion area n = 6. H, Representative picrosirius red staining of aortic root lesions with bars indicating fibrous cap thickness and quantification of fibrous cap thickness n = 6. All scale bar = 300um. ****P<0.0001, ***P<0.001, ** P<0.01, *P<0.05 by t-test.

Figure 2. ADAMTS7 promotes foam cell expansion. A, Flow cytometry based quantification of foam cells through LipidTOX staining of the aorta. A normolipidemic aorta was used to establish the LipidTOX high gate. B, Breakdown of foam cells that stained positively for CD11B and CD64. C, Foam cell analysis with the SMC lineage tracer ZsGreen and leukocyte marker CD45 n = 4-6 mice. D, In vitro foam cell analysis with primary cells treated with 10ug/mL Dil-oxLDL for 24 hours, n = 3. ** P<0.01, *P<0.05 by t-test.

Figure 3. Bulk RNAseq of TG+ primary SMCs reveals an increase in lipid handling genes. A, Volcano plot of the most upregulated and downregulated genes (by *P* value adjusted for multiple comparisons). Passage two cells were used for RNAseq. B, qRT-PCR confirmation of upregulated lipid uptake and macrophage-like genes n = 4. Normalization was performed relative to *Hprt1*. C, Ingenuity Pathway Analysis of differentially expressed genes with Ingenuity Canonical Pathways highlighted. Shown pathways are predicted to be upregulated within TG+ primary SMCs. D, Confirmation of enhanced SMC CD36 in vivo. Flow cytometry analysis of lineage traced mice after 12 weeks of WTD feeding n = 4- 6 mice. Flow plots are shown after gating for cells, singlet, and live cell (DAPI negative). ****P<0.0001, ***P<0.001, ** P<0.01, *P<0.05 by t-test.

Figure 4. CD36 and PU.1 mediate ADAMTS7 conferred foam cell expansion. A, Confirmation of knockdown of *Cd36* through siRNA. Primary SMCs were treated with 10nM of either an NTC or *Cd36* siRNA. Knockdown was assessed 48 hours after transfection n = 3-5. B, Flow analysis of oxLDL lipid uptake. 24 hours post siRNA transfection, cells were treated with 10ug/mL of DIL-oxLDL, and uptake was assessed 24 hours post oxLDL treatment n = 3. C, Knockdown of *Spi1* in primary SMCs. Cells were treated with 10nM of siRNA, and 48 hours after transfection, cells were harvested for qRT-PCR. D, Flow analysis of oxLDL lipid uptake. 24 hours post *Spi1* siRNA transfection, cells were treated with 10ug/mL of DIL-oxLDL, and uptake was assessed 24 hours post oxLDL treatment ****P<0.0001, ***P<0.001, ** P<0.01, *P<0.05 Statistics were analyzed by two-way ANOVA with Sidak's multiple comparison test.

Figure 5. Identifying endogenous ADAMTS7 expression. A, Single Cell RNA-sequencing of human carotid atherosclerosis and cell clustering identities. B, RNAscope of the brachial cephalic artery after WTD feeding. Nuclei are stained with DAPI. Scale bar = 100um C and D, RNAscope of the brachial cephalic artery of *Ldlr-/-* mice after seven and ten weeks of WTD feeding and probed against *Adamts7* and *Pecam1*. White arrows highlight endothelial cell expression of *Adamts7*. Yellow arrows indicate non-endothelial cell expression of Adamts7. Scale bar = 50um.

Figure 6. SMC knockout of *Adamts7* and endothelial cell transgenic *Adamts7*. A, Schematic outlining the construct of the conditional knockout allele with exons 5 and 6 floxed. B, Representative Oil Red O staining of en face aortas and enumeration. C, Cholesterol and weights of endothelial cell transgenic mice after 16 weeks of WTD feeding n = 3-4 female mice. D, Oil Red O staining of the en face aorta and quantification of lesion area E, Flow cytometry based quantification of foam cells through LipidTOX staining of the aorta. A normolipidemic aorta was used to establish the LipidTOX high gate. n = 3-4. F, Foam cell analysis with staining for the leukocyte marker CD45 n = 3-4 mice.*P<0.05 by t-test.

Table 1. IPA upstream regulator analysis to identify candidate transcription factors. Upstream regulator analysis of RNAseq reveals activated candidate molecules responsible for the gene expression changes. Five transcription factors are listed within the top 25 listed molecules.

Figure S1. Weights and cholesterol of TG mice Mice's weight (g) and plasma total cholesterol (mg/dL) after 16 weeks of WTD feeding. Statistics were analyzed by t-test.

Figure S2. Increased atherosclerosis with short durations of WTD feeding in TG+ mice.

Representative images of oil red o stained en face aortas after three, six, and nine weeks of WTD feeding. *P□<□0.05; ***P□<□0.001 by t-test.

Figure S3. Knockdown of candidate transcription factors does not alter *Adamts7* conferred macrophage-like and lipid-handling genes.

Indicated siRNAs (10nM) were used to knock down candidate transcription factors in primary SMCs from TG- and TG+ mice. 48 hours after transfection, cells were harvested for qRT-PCR analysis. ****P<0.0001, ***P<0.001, ** P<0.01, *P<0.05 by two-way ANOVA with Sidak's multiple comparison test.

REFERENCE

1 Tsao, C. W. *et al.* Heart Disease and Stroke Statistics-2023 Update: A Report From the American Heart Association. *Circulation*, doi:10.1161/CIR.0000000000001123 (2023).

2 Aragam, K. G. *et al.* Discovery and systematic characterization of risk variants and genes for coronary artery disease in over a million participants. *Nat Genet* **54**, 1803-1815, doi:10.1038/s41588-022-01233-6 (2022).

3 Nikpay, M. *et al.* A comprehensive 1,000 Genomes-based genome-wide association meta-analysis of coronary artery disease. *Nat Genet* **47**, 1121-1130, doi:10.1038/ng.3396 (2015).

4 Reilly, M. P. *et al.* Identification of ADAMTS7 as a novel locus for coronary atherosclerosis and association of ABO with myocardial infarction in the presence of coronary atherosclerosis: two genome-wide association studies. *Lancet* **377**, 383-392, doi:10.1016/S0140-6736(10)61996-4 (2011).

5 Schunkert, H. *et al.* Large-scale association analysis identifies 13 new susceptibility loci for coronary artery disease. *Nat Genet* **43**, 333-338, doi:10.1038/ng.784 (2011).

6 Luan, Y. *et al.* Inhibition of ADAMTS-7 and ADAMTS-12 degradation of cartilage oligomeric matrix protein by alpha-2-macroglobulin. *Osteoarthritis Cartilage* **16**, 1413-1420, doi:10.1016/j.joca.2008.03.017 (2008).

7 Bauer, R. C. *et al.* Knockout of Adamts7, a novel coronary artery disease locus in humans, reduces atherosclerosis in mice. *Circulation* **131**, 1202-1213, doi:10.1161/CIRCULATIONAHA.114.012669 (2015).

8 Chung, A., Reilly, M. P. & Bauer, R. C. ADAMTS7: a Novel Therapeutic Target in Atherosclerosis. *Curr Atheroscler Rep* **25**, 447-455, doi:10.1007/s11883-023-01115-0 (2023).

9 Mizoguchi, T. *et al.* Coronary Disease Association With ADAMTS7 Is Due to Protease Activity. *Circ Res* **129**, 458-470, doi:10.1161/CIRCRESAHA.121.319163 (2021).

10 Ma, Z. *et al.* Peptide Vaccine Against ADAMTS-7 Ameliorates Atherosclerosis and Postinjury Neointima Hyperplasia. *Circulation*, doi:10.1161/CIRCULATIONAHA.122.061516 (2022).

11 Wang, L. *et al.* ADAMTS-7 mediates vascular smooth muscle cell migration and neointima formation in balloon-injured rat arteries. *Circ Res* **104**, 688-698, doi:10.1161/CIRCRESAHA.108.188425 (2009).

12 Pan, H. *et al.* Single-Cell Genomics Reveals a Novel Cell State During Smooth Muscle Cell Phenotypic Switching and Potential Therapeutic Targets for Atherosclerosis in Mouse and Human. *Circulation* **142**, 2060-2075, doi:10.1161/CIRCULATIONAHA.120.048378 (2020).

13 Wang, Y. *et al.* Smooth Muscle Cells Contribute the Majority of Foam Cells in ApoE (Apolipoprotein E)-Deficient Mouse Atherosclerosis. *Arterioscler Thromb Vasc Biol* **39**, 876-887, doi:10.1161/ATVBAHA.119.312434 (2019).

14 Wirth, A. *et al.* G12-G13-LARG-mediated signaling in vascular smooth muscle is required for salt-induced hypertension. *Nat Med* **14**, 64-68, doi:10.1038/nm1666 (2008).
15 Chattopadhyay, A. *et al.* Cholesterol-Induced Phenotypic Modulation of Smooth Muscle Cells to Macrophage/Fibroblast-like Cells Is Driven by an Unfolded Protein Response. *Arterioscler Thromb Vasc Biol* **41**, 302-316, doi:10.1161/ATVBAHA.120.315164 (2021).
16 Jay, A. G., Chen, A. N., Paz, M. A., Hung, J. P. & Hamilton, J. A. CD36 binds oxidized low density lipoprotein (LDL) in a mechanism dependent upon fatty acid binding. *J Biol Chem* **290**, 4590-4603, doi:10.1074/jbc.M114.627026 (2015).
17 McKercher, S. R. *et al.* Targeted disruption of the PU.1 gene results in multiple hematopoietic abnormalities. *EMBO J* **15**, 5647-5658 (1996).
18 Bashore, A. C. *et al.* High-Dimensional Single-Cell Multimodal Landscape of Human Carotid Atherosclerosis. *medRxiv*, doi:10.1101/2023.07.13.23292633 (2023).
19 Austin, C. P. *et al.* The knockout mouse project. *Nat Genet* **36**, 921-924, doi:10.1038/ng0904-921 (2004).
20 Pu, X. *et al.* ADAMTS7 cleavage and vascular smooth muscle cell migration is affected by a coronary-artery-disease-associated variant. *Am J Hum Genet* **92**, 366-374, doi:10.1016/j.ajhg.2013.01.012 (2013).
21 Tcheandjieu, C. *et al.* Large-scale genome-wide association study of coronary artery disease in genetically diverse populations. *Nat Med* **28**, 1679-1692, doi:10.1038/s41591-022-01891-3 (2022).
22 Sharma, D. *et al.* Comprehensive Integration of Multiple Single-Cell Transcriptomic Data Sets Defines Distinct Cell Populations and Their Phenotypic Changes in Murine Atherosclerosis. *Arterioscler Thromb Vasc Biol* **44**, 391-408, doi:10.1161/ATVBAHA.123.320030 (2024).
23 Inaba, T. *et al.* Transcription factor PU.1 mediates induction of c-fms in vascular smooth muscle cells: a mechanism for phenotypic change to phagocytic cells. *Mol Cell Biol* **16**, 2264-2273, doi:10.1128/MCB.16.5.2264 (1996).
24 Dubland, J. A. *et al.* Low LAL (Lysosomal Acid Lipase) Expression by Smooth Muscle Cells Relative to Macrophages as a Mechanism for Arterial Foam Cell Formation. *Arterioscler Thromb Vasc Biol* **41**, e354-e368, doi:10.1161/ATVBAHA.120.316063 (2021).
25 Miller, C. L. & Zhang, H. Clarifying the Distinct Roles of Smooth Muscle Cell-Derived Versus Macrophage Foam Cells and the Implications in Atherosclerosis. *Arterioscler Thromb Vasc Biol* **41**, 2035-2037, doi:10.1161/ATVBAHA.121.316287 (2021).
26 Kim, K. *et al.* Transcriptome Analysis Reveals Nonfoamy Rather Than Foamy Plaque Macrophages Are Proinflammatory in Atherosclerotic Murine Models. *Circ Res* **123**, 1127-1142, doi:10.1161/CIRCRESAHA.118.312804 (2018).
27 Bengtsson, E. *et al.* ADAMTS-7 is associated with a high-risk plaque phenotype in human atherosclerosis. *Sci Rep* **7**, 3753, doi:10.1038/s41598-017-03573-4 (2017).
28 Sharifi, M. A. *et al.* ADAMTS-7 Modulates Atherosclerotic Plaque Formation by Degradation of TIMP-1. *Circ Res* **133**, 674-686, doi:10.1161/CIRCRESAHA.123.322737 (2023).
29 Sorensen, I., Adams, R. H. & Gossler, A. DLL1-mediated Notch activation regulates endothelial identity in mouse fetal arteries. *Blood* **113**, 5680-5688, doi:10.1182/blood-2008-08-174508 (2009).
30 Ostriker, A. C. *et al.* TET2 Protects Against Vascular Smooth Muscle Cell Apoptosis and Intimal Thickening in Transplant Vasculopathy. *Circulation* **144**, 455-470, doi:10.1161/CIRCULATIONAHA.120.050553 (2021).

FIGURE 1

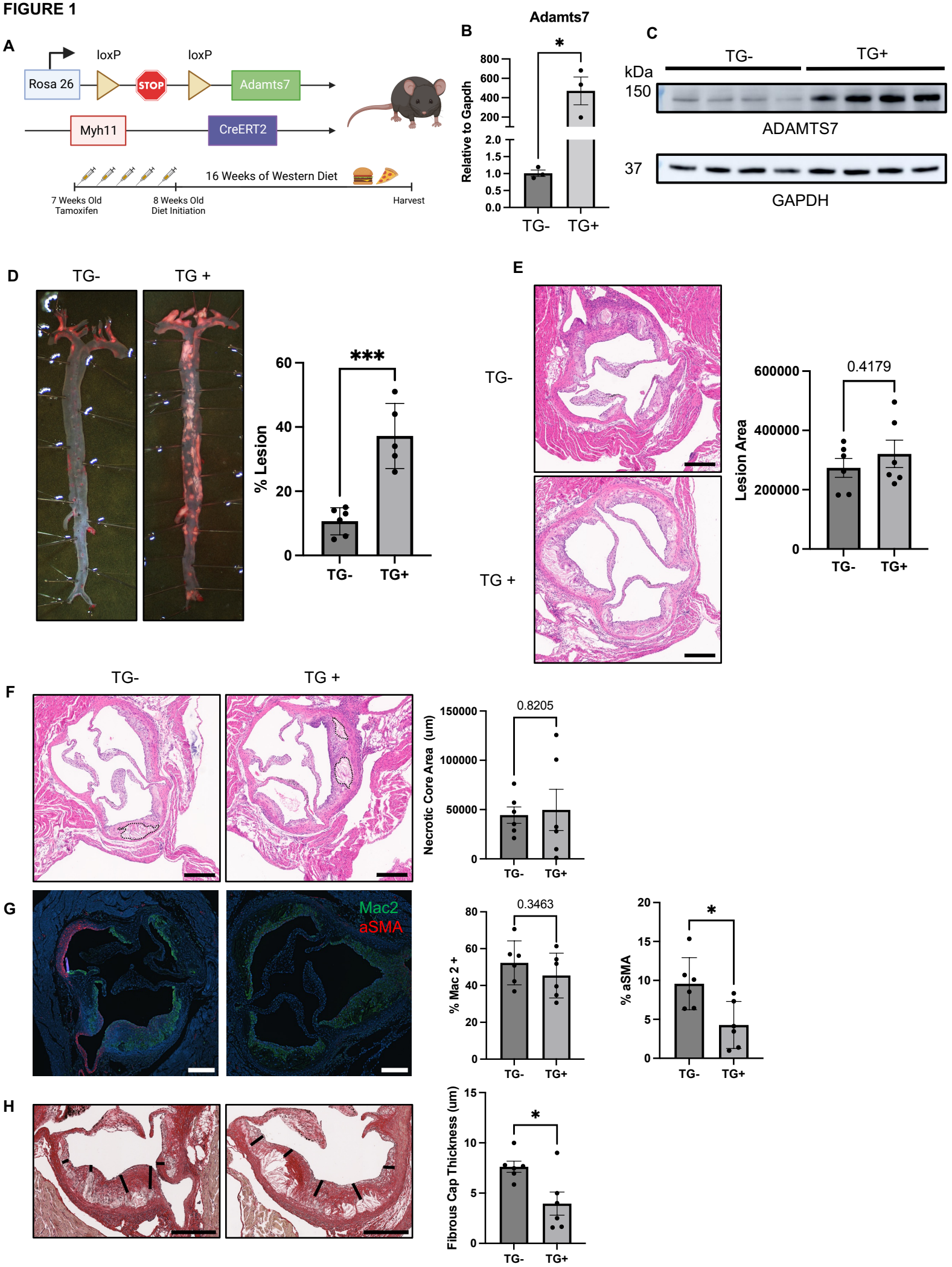
A
loxP
loxP
Rosa 26
STOP
Adamts7
Myh11
CreERT2
16 Weeks of Western Diet
7 Weeks Old
Tamoxifen
8 Weeks Old
Diet Initiation
Harvest
B
Adamts7
Relative to Gapdh
TG-
TG+
C
TG-
TG+
kDa
150
ADAMTS7
37
GAPDH
D
TG-
TG +
% Lesion
TG-
TG+
E
TG-
TG +
Lesion Area
0.4179
TG-
TG+
F
TG-
TG +
Necrotic Core Area (um)
0.8205
TG-
TG+
G
Mac2
aSMA
% Mac 2 +
0.3463
TG-
TG+
% aSMA
TG-
TG+
H
Fibrous Cap Thickness (um)
TG-
TG+

FIGURE 2

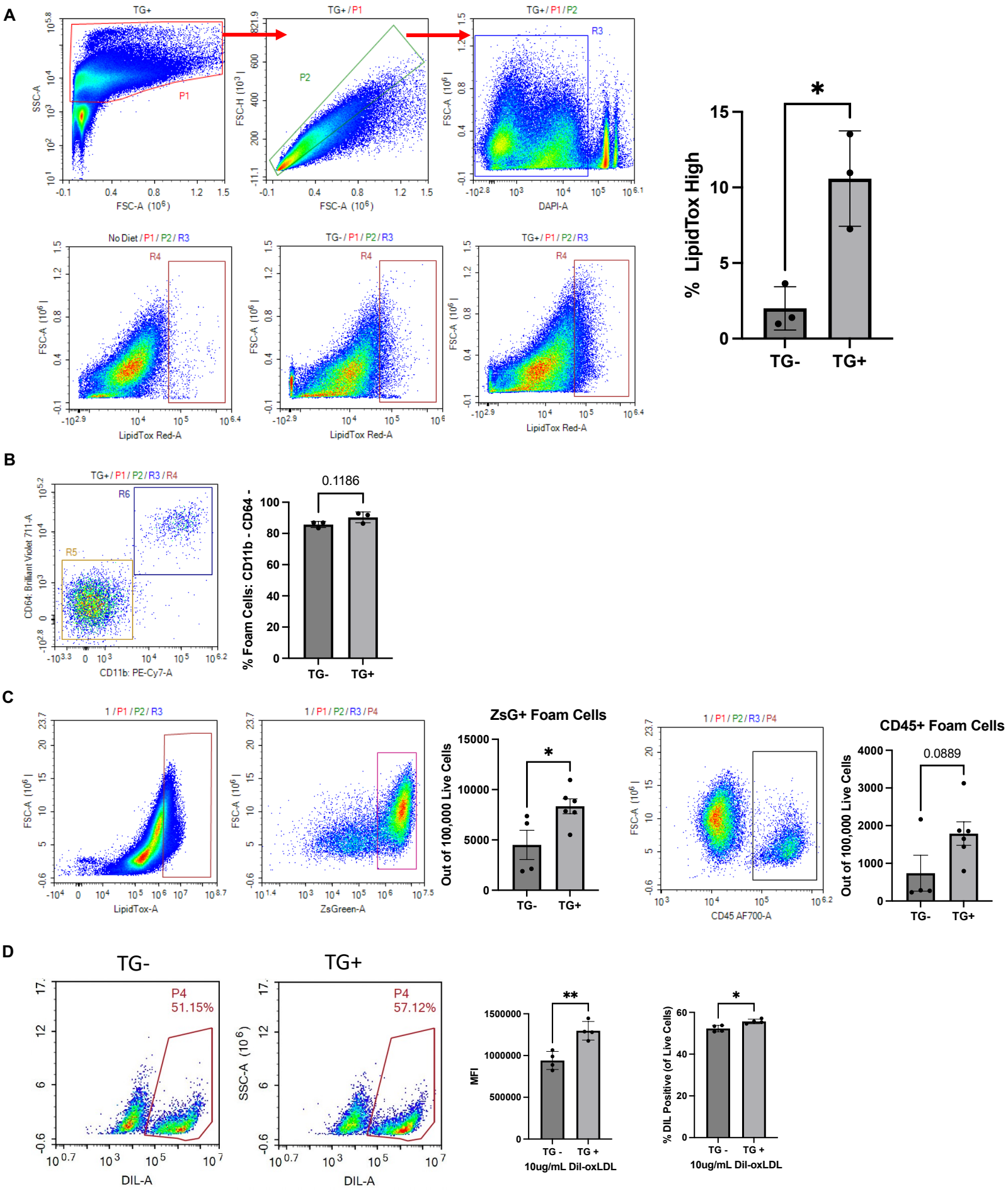
A
TG+
P1
SSC-A
FSC-A (10^6)
TG+ / P1
P2
FSC-H (10^3)
TG+ / P1 / P2
R3
DAPI-A
No Diet / P1 / P2 / R3
R4
LipidTox Red-A
TG- / P1 / P2 / R3
TG+ / P1 / P2 / R3
% LipidTox High
TG-
TG+
B
TG+ / P1 / P2 / R3 / R4
R6
R5
CD64: Brilliant Violet 711-A
CD11b: PE-Cy7-A
0.1186
% Foam Cells: CD11b - CD64 -
C
1 / P1 / P2 / R3
LipidTox-A
1 / P1 / P2 / R3 / P4
ZsGreen-A
ZsG+ Foam Cells
Out of 100,000 Live Cells
CD45 AF700-A
CD45+ Foam Cells
0.0889
D
TG-
TG+
P4
51.15%
57.12%
SSC-A (10^6)
DIL-A
MFI
TG -
TG +
10ug/mL Dil-oxLDL
% DIL Positive (of Live Cells)

FIGURE 3

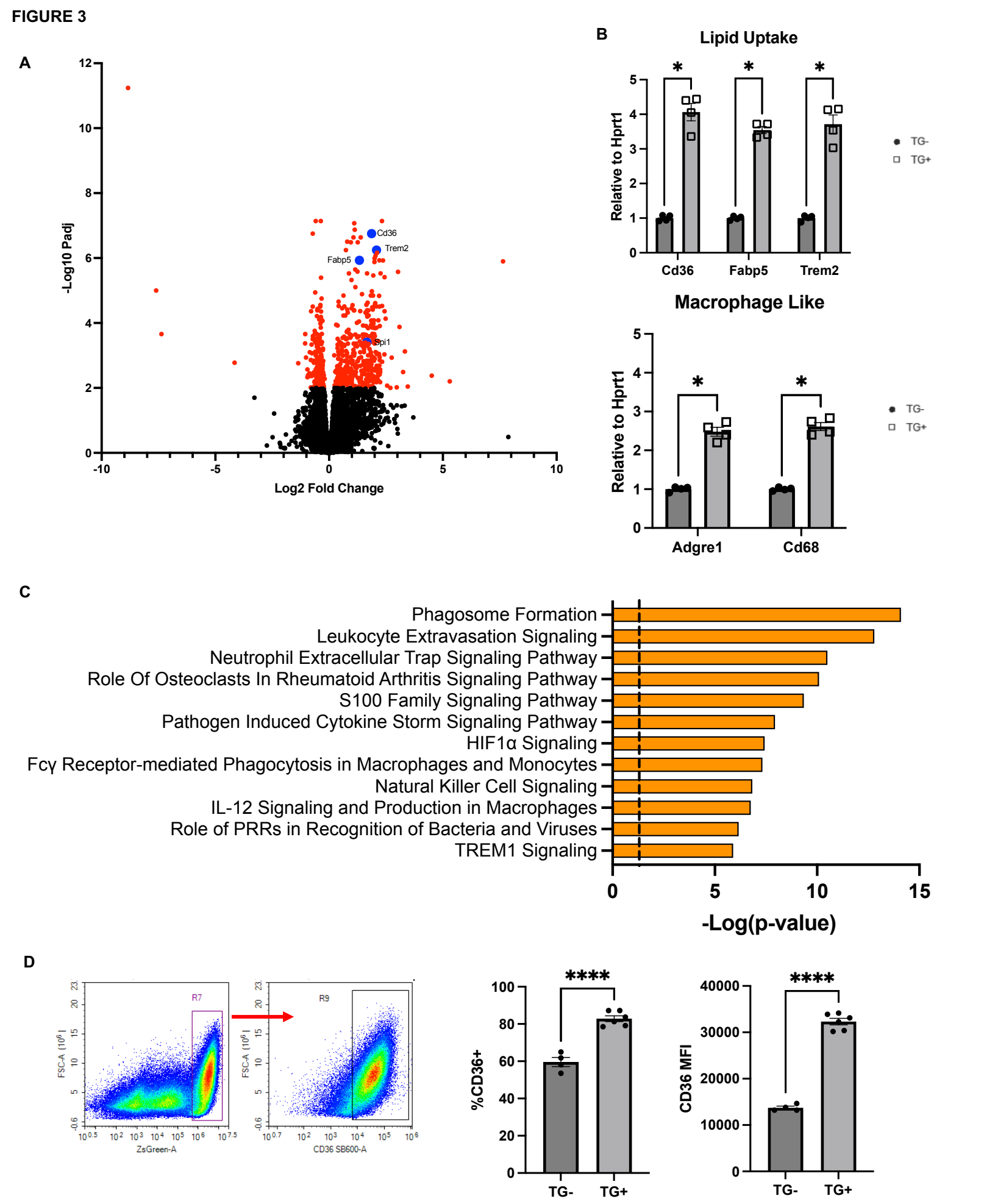
A
-Log10 Padj
Log2 Fold Change
Cd36
Trem2
Fabp5
Spi1
B
Lipid Uptake
Relative to Hprt1
Cd36
Fabp5
Trem2
TG-
TG+
Macrophage Like
Adgre1
Cd68
C
Phagosome Formation
Leukocyte Extravasation Signaling
Neutrophil Extracellular Trap Signaling Pathway
Role Of Osteoclasts In Rheumatoid Arthritis Signaling Pathway
S100 Family Signaling Pathway
Pathogen Induced Cytokine Storm Signaling Pathway
HIF1α Signaling
Fcγ Receptor-mediated Phagocytosis in Macrophages and Monocytes
Natural Killer Cell Signaling
IL-12 Signaling and Production in Macrophages
Role of PRRs in Recognition of Bacteria and Viruses
TREM1 Signaling
-Log(p-value)
D
R7
R9
ZsGreen-A
CD36 SB600-A
%CD36+
CD36 MFI
****

FIGURE 4

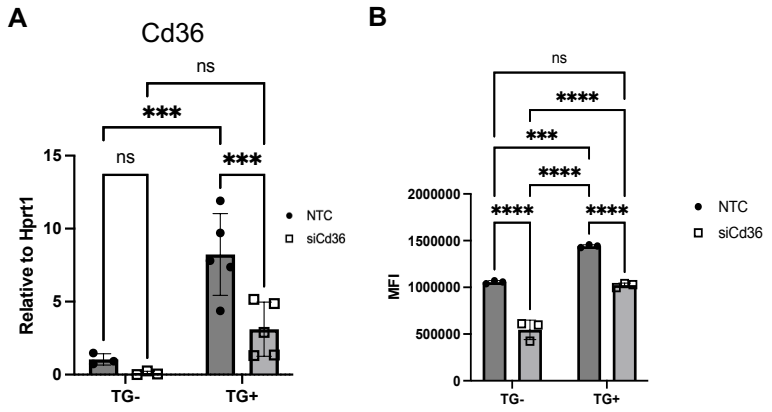
A
Cd36
ns
***
ns
***
15
10
5
0
Relative to Hprt1
NTC
siCd36
TG-
TG+
B
ns
****
***
****
****
****
2000000
1500000
1000000
500000
0
MFI
NTC
siCd36
TG-
TG+

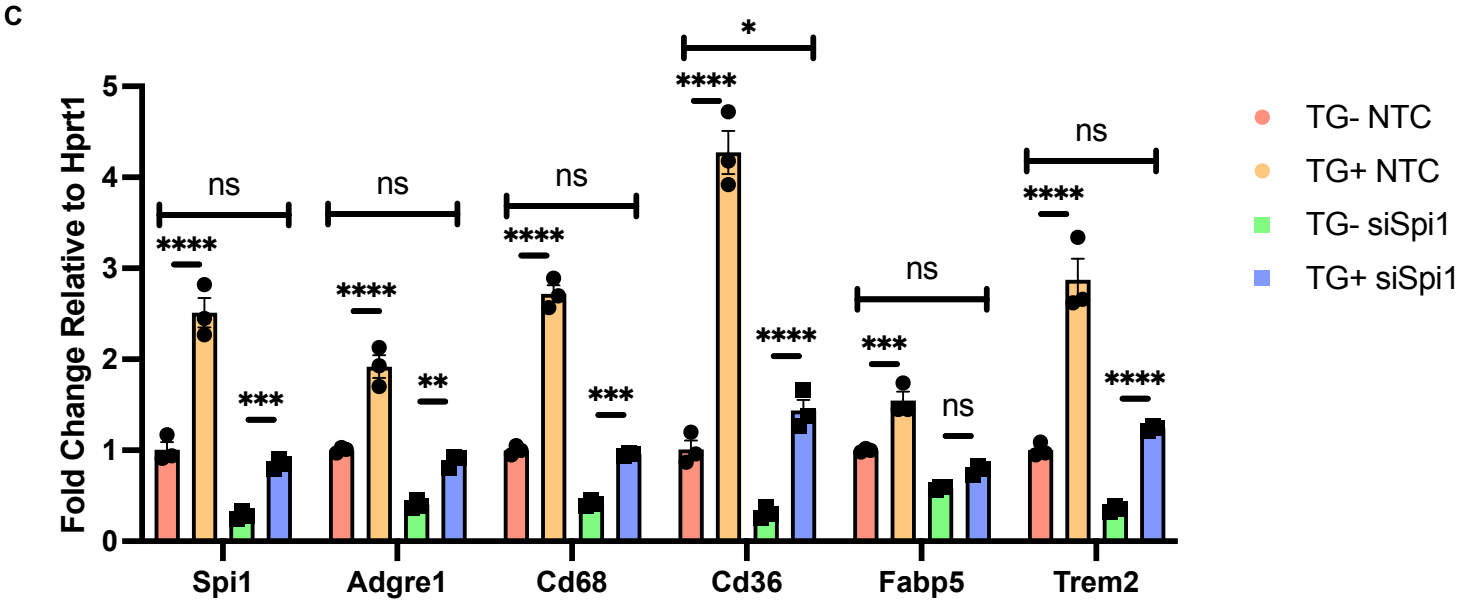
C
Fold Change Relative to Hprt1
5
4
3
2
1
0
ns
****
***
ns
****
**
ns
****
***
*
****
****
ns
***
ns
ns
****
****
Spi1
Adgre1
Cd68
Cd36
Fabp5
Trem2
TG- NTC
TG+ NTC
TG- siSpi1
TG+ siSpi1

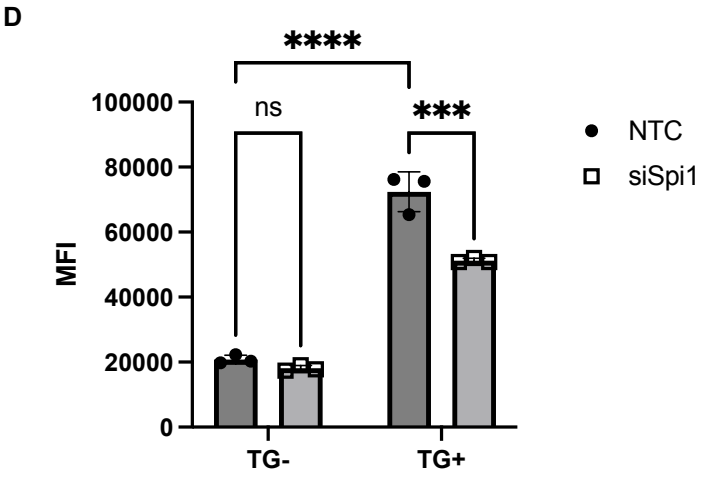
D
****
ns
***
100000
80000
60000
40000
20000
0
MFI
TG-
TG+
NTC
siSpi1

FIGURE 5

A

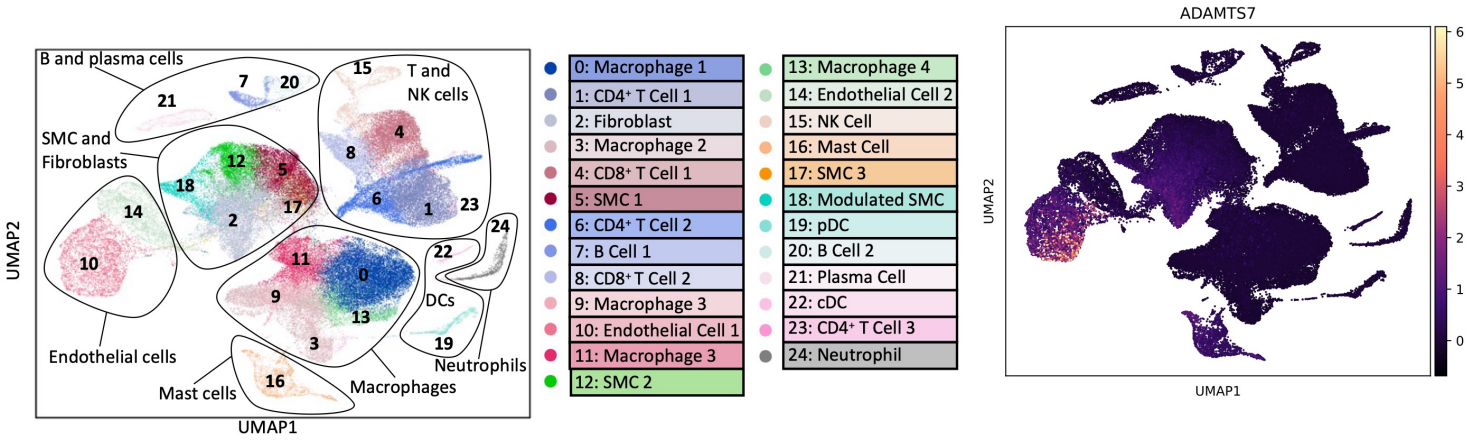

B

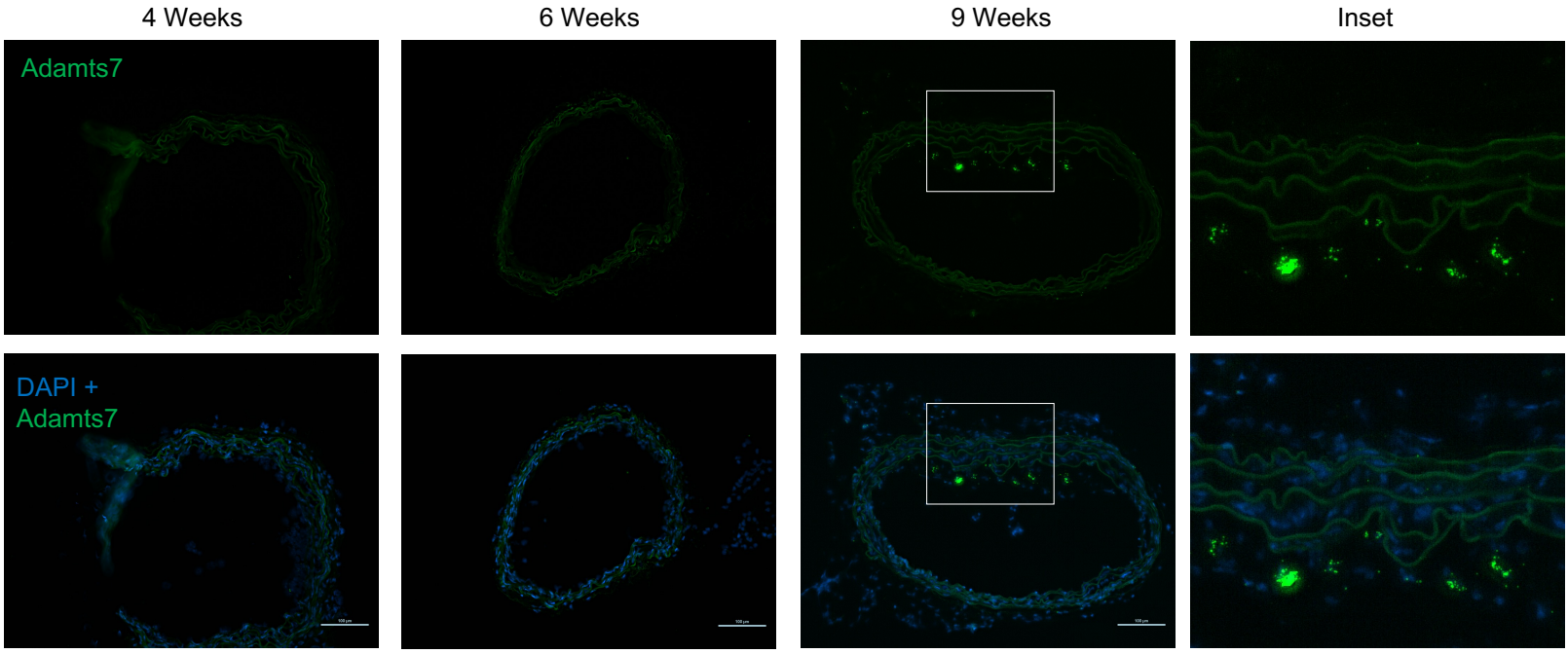

C

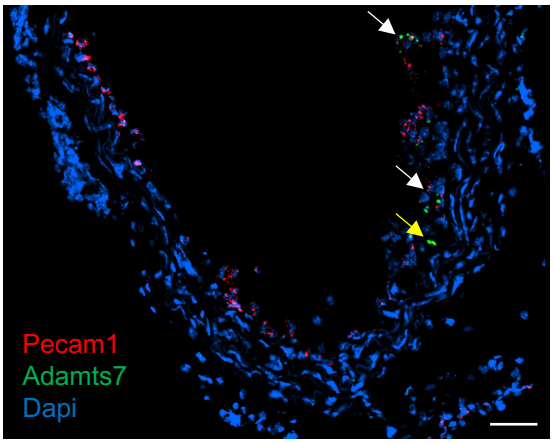

D

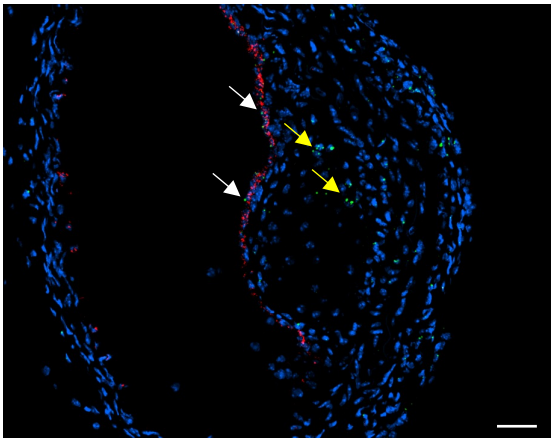

FIGURE 6

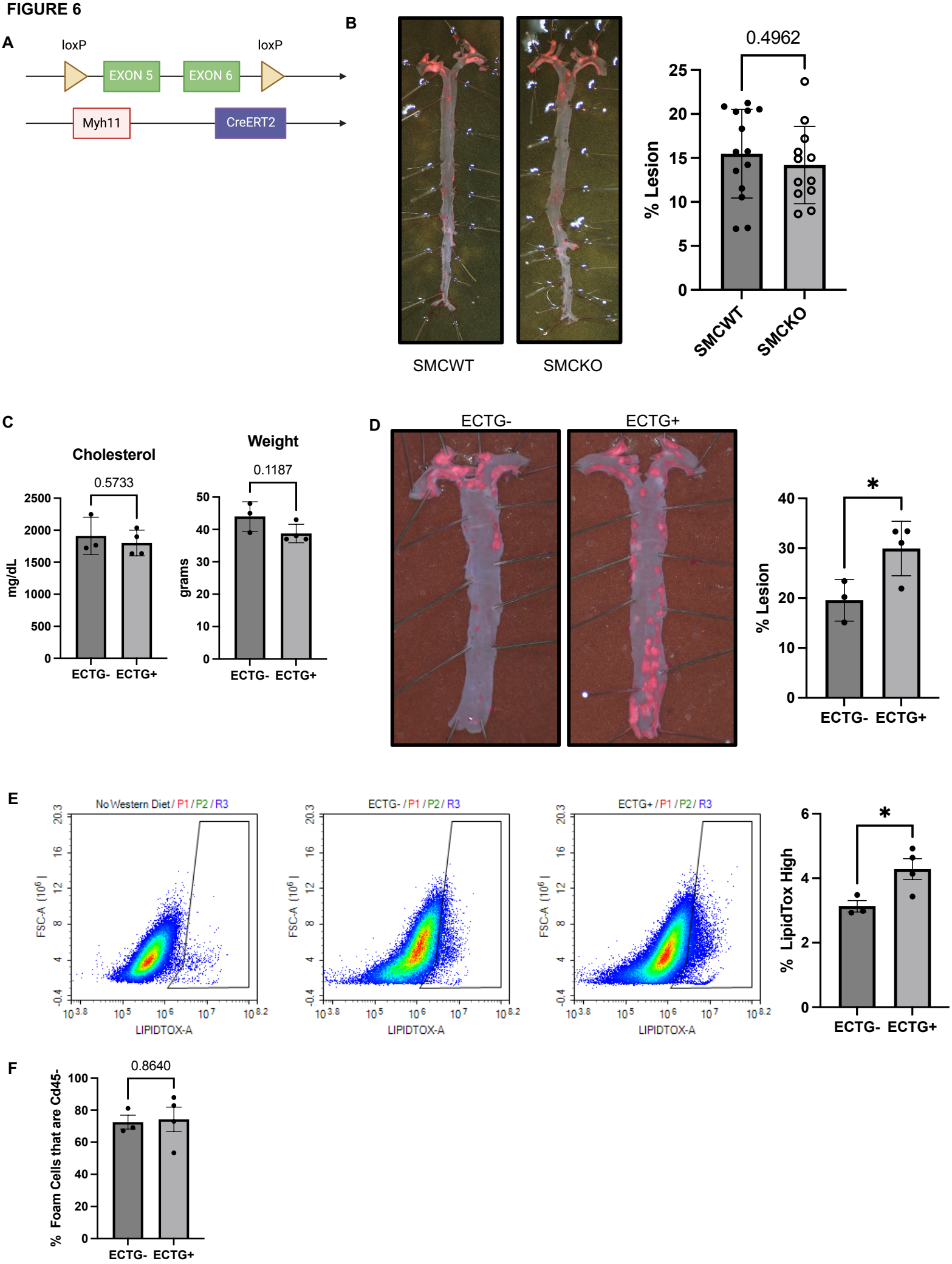
A
loxP
loxP
EXON 5
EXON 6
Myh11
CreERT2
B
SMCWT
SMCKO
0.4962
% Lesion
25
20
15
10
5
0
SMCWT
SMCKO
C
Cholesterol
0.5733
mg/dL
2500
2000
1500
1000
500
0
ECTG-
ECTG+
Weight
0.1187
grams
50
40
30
20
10
0
ECTG-
ECTG+
D
ECTG-
ECTG+
*
% Lesion
40
30
20
10
0
ECTG-
ECTG+
E
No Western Diet / P1 / P2 / R3
ECTG- / P1 / P2 / R3
ECTG+ / P1 / P2 / R3
FSC-A (10^6)
LIPIDTOX-A
*
% LipidTox High
6
4
2
0
ECTG-
ECTG+
F
0.8640
% Foam Cells that are Cd45-
100
80
60
40
20
0
ECTG-
ECTG+

SUPPLEMENTARY FIGURE 1

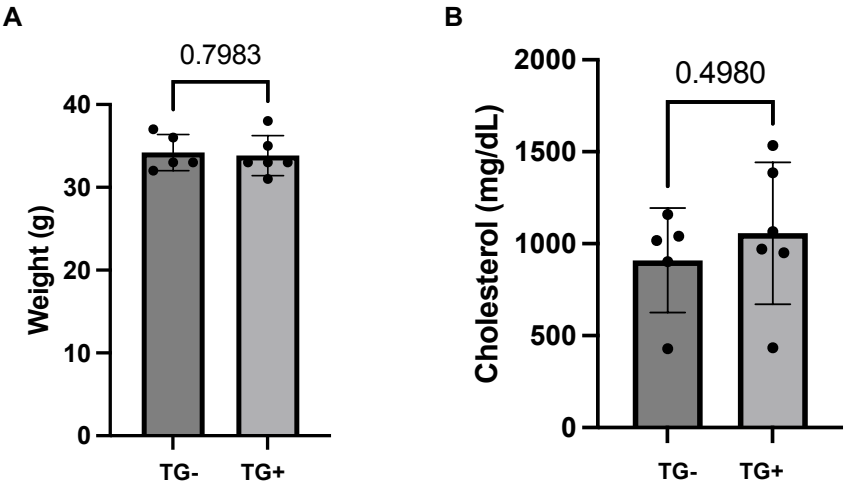

SUPPLEMENTARY FIGURE 2

A

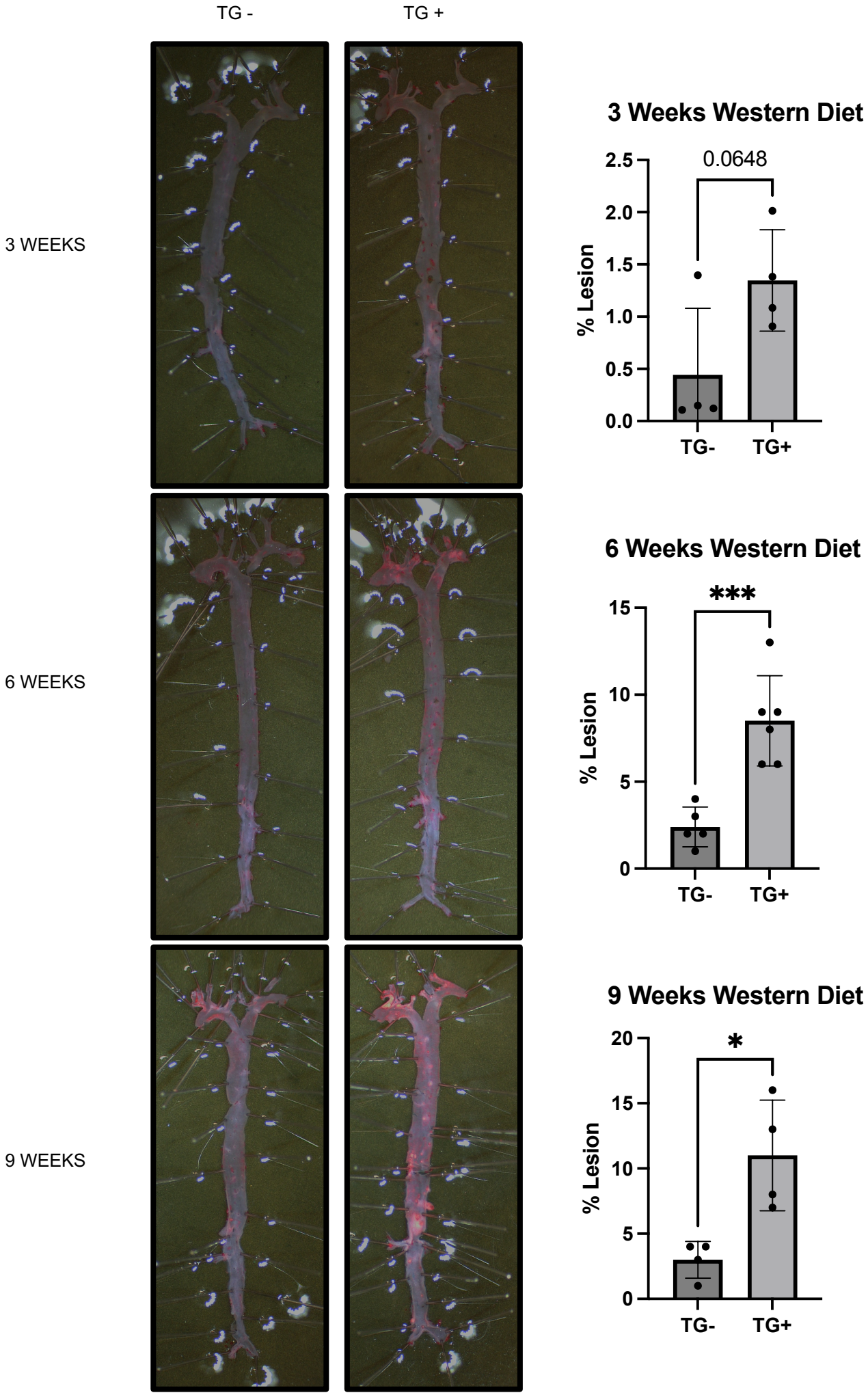
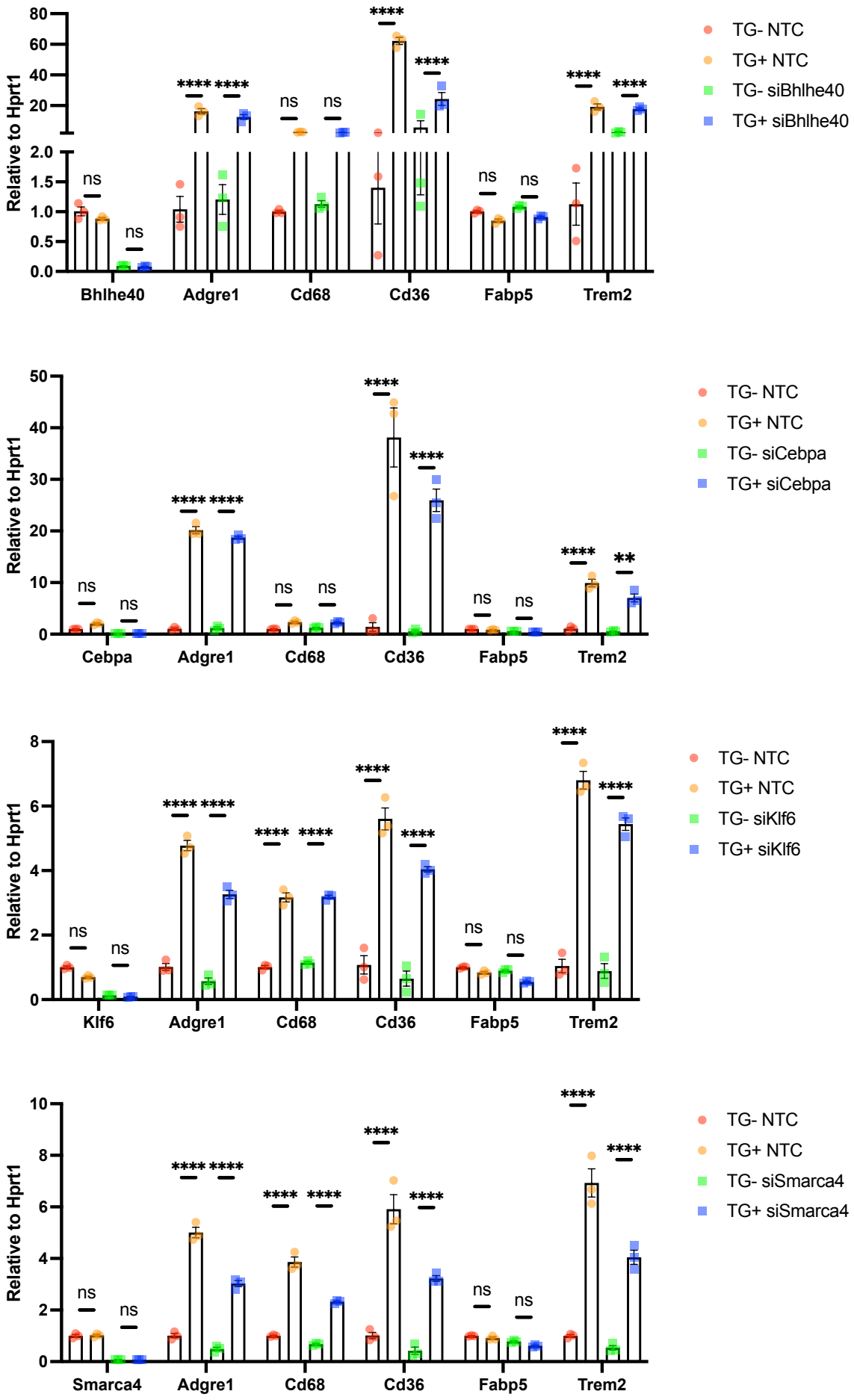
SUPPLEMENTARY FIGURE 3